

# UNCLASSIFIED

|   |
|---|
|   |
|   |
|   |
| AD NUMBER   |
| AD463879  |
| NEW LIMITATION CHANGE   |
| TO<br>Approved for public release, distribution unlimited   |
| FROM<br>Distribution authorized to U.S. Gov't. agencies and their contractors; Administrative/Operational Use; APR 1965. Other requests shall be referred to US Office of Naval Research, 800 North Quincy Street, Arlington, VA. |
| AUTHORITY   |
| ONR ltr, 9 Nov 1977   |

THIS PAGE IS UNCLASSIFIED

THIS REPORT HAS BEEN DELIMITED  
AND CLEARED FOR PUBLIC RELEASE  
UNDER DOD DIRECTIVE 5200.20 AND  
NO RESTRICTIONS ARE IMPOSED UPON  
ITS USE AND DISCLOSURE.

DISTRIBUTION STATEMENT A

APPROVED FOR PUBLIC RELEASE;  
DISTRIBUTION UNLIMITED.

UNCLASSIFIED

AD 4 6 3 8 7 9

DEFENSE DOCUMENTATION CENTER

FOR

SCIENTIFIC AND TECHNICAL INFORMATION

CAMERON STATION ALEXANDRIA, VIRGINIA



UNCLASSIFIED

NOTICE: When government or other drawings, specifications or other data are used for any purpose other than in connection with a definitely related government procurement operation, the U. S. Government thereby incurs no responsibility, nor any obligation whatsoever; and the fact that the Government may have formulated, furnished, or in any way supplied the said drawings, specifications, or other data is not to be regarded by implication or otherwise as in any manner licensing the holder or any other person or corporation, or conveying any rights or permission to manufacture, use or sell any patented invention that may in any way be related thereto.

FOR ERRATA

AD 463879

THE FOLLOWING PAGES ARE CHANGES

TO BASIC DOCUMENT

CALIFORNIA INSTITUTE OF TECHNOLOGY

PASADENA, CALIFORNIA 91109

HYDRODYNAMICS LABORATORY

KARMAN LABORATORY OF  
FLUID MECHANICS AND JET PROPULSION

May 26, 1965

Recipients of California  
Institute of Technology  
Hydrodynamics Laboratory  
Report No. 111.3

SUBJECT Errata for Report No. 111.3

Gentlemen:

It is requested that the following changes be made in your copy of California Institute of Technology Hydrodynamics Laboratory Report No. 111.3, entitled "The Wall Effect In Cavity Flow," by D. K. Ai and Z. L. Harrison, dated April 1965:

The information in the caption of Fig. 10 should appear with Fig. A-2.

The information in the caption of Fig. A-2 should appear with Fig. 10.

Very truly yours,

*Mary E. Goodwin*  
Mary E. Goodwin

463879

4 5 6 3 8 7 9

1

Best Available Copy

Office of Naval Research  
Department of the Navy  
Contract Nonr-220(41)

THE WALL EFFECT IN CAVITY FLOW

by

Daniel K. Ai

and

Z. L. Harrison

Reproduction in whole or in part is permitted for  
any purpose of the United States Government

Hydrodynamics Laboratory  
Karman Laboratory of Fluid Mechanics and Jet Propulsion  
California Institute of Technology  
Pasadena, California

Report No. 111.3

Approved by: T. Y. Wu  
April 1965



## ABSTRACT

A non-linear theory for the calculation of the flow field of an oblique flat plate under blockage condition is given using the techniques of integral equations. Numerical results are obtained with the aid of a high speed digital computer for the plate situated mid-channel at values of the angle of attack from  $5^{\circ}$  to  $90^{\circ}$  and the channel width-chord ratio from 3 to 20. Also obtained are results for the plate situated at two different off-center positions for a channel width-chord ratio 5 and angles of attack less than  $30^{\circ}$ .

## NOMENCLATURE

|                 |  |
|-----------------|--|
| $A$             | = leading edge of the plate; origin of the coordinate system.                      |
| $B$             | = trailing edge of the plate; $x = 1$ .  |
| $C$             | = scale factor.  |
| $C_D$           | = drag coefficient.  |
| $C_L$           | = lift coefficient.  |
| $D$             | = stagnation point on the plate.   |
| $F_D$           | = drag force.  |
| $f$             | = complex potential.   |
| $H_A$           | = normal distance from $A$ to the upper channel wall.                              |
| $H_1, H_2$      | = widths of the flow above and below the dividing streamline at upstream infinity. |
| $h_1, h_2$      | = widths of the flow above and below the cavity at downstream infinity.            |
| $I$             | = flow at upstream infinity.   |
| $J$             | = flow at downstream infinity between the upper cavity and channel wall.           |
| $K$             | = flow at downstream infinity between the lower channel and cavity wall.           |
| $k_0, k_1, k_2$ | = parameters in the transformation.  |
| $p_\infty$      | = free stream pressure.  |
| $p_c$           | = cavity pressure.   |
| $U, V$          | = uniform up- and downstream velocities respectively.                              |
| $W$             | = channel width = $H_1 + H_2$ .  |
| $w$             | = complex velocity.  |
| $z$             | = $x + iy$ , the physical plane.   |
| $\alpha$        | = angle of attack.   |
| $\sigma$        | = $(p_\infty - p_c)/\frac{1}{2} \rho U^2$ , cavitation number.                     |
| $\rho$          | = density of the liquid.   |
| $\theta$        | = direction of the flow.   |

## Introduction

The two-dimensional cavity theory of an unbounded fluid, with the recently published works<sup>(1), (2)</sup> on the non-linear solution of bodies of general shape, can be considered a well established field. For an experimentalist who has to perform the tests, however, the existing theories cannot always be applied directly and have to be modified mainly because the flow one creates for experiment is often bounded by different types of boundaries. These boundaries can be free surfaces of constant pressure if the equipment in use is a jet, rigid walls if it is a water tunnel, or both if it is a free surface channel. The essential problem is to determine the effect of the boundaries. In the past, many papers have been published on this problem. A small portion of these are listed here as references<sup>(3), (4), (5), (6)</sup>. We shall not repeat what they have done since these references are available and well known. This paper also deals with this problem, but the interest is focused only on the unsymmetric flow for arbitrary angle of attack and the boundaries considered are rigid walls. In a subsequent report, we shall treat the cases of the free jet and the free surface channel.

It is a well known fact that the cavity length behind a body depends essentially on  $\sigma$ , an important parameter known as the cavitation number and defined as

$$\sigma = (p_{\infty} - p_c) / \frac{1}{2} \rho U^2. \quad (1)$$

Here  $p_{\infty}$  is the free stream pressure,  $U$  the free stream velocity, and  $p_c$  is the cavity pressure presumably nearly constant. In general, the length would increase as  $\sigma$  decreases and with the presence of free surfaces, e. g. in a jet,  $\sigma$  would become zero when the length approaches infinity. However, this phenomenon is not observed in a water tunnel with rigid walls. In this case  $\sigma$  would reach a finite positive limit  $\sigma_c$  as the cavity length increases indefinitely hence cavitation numbers below  $\sigma_c$  are not attainable. Thus not all cavity flow conditions can be modeled in a water tunnel. The phenomenon corresponding to  $\sigma = \sigma_c$  in a water tunnel is called blockage or choking and the determination of  $\sigma_c$  is therefore one of the central problems in water tunnel testing of cavity flows.

In this paper, the two-dimensional non-linear theory of a choked unsymmetrical flow over a flat plate at an arbitrary angle of attack is worked out using the techniques of integral equations. Numerical results are obtained on a high speed digital computer (IBM 7094).

#### Formulation of the problem and preliminary calculations.

Consider the idealized cavity flow in a water tunnel with rigid walls, depicted in Fig. 1. We assume a uniform upstream flow with velocity  $U$ , and a uniform downstream velocity  $V$  as the cavity, which has a stationary interface, approaches its maximum cross-section. The flat plate, set at an arbitrary angle of attack, can be located anywhere in the tunnel and the stream after impinging on the frontal side of the plate separates smoothly at both its leading and trailing edges. The plate is of length unity or one may say all dimensions are normalized by the chord. The coordinate axes are set normal and parallel to the plate with the origin at the leading edge.

If we call  $\bar{w}$ , the velocity vector, with magnitude  $|w|$  and direction  $\theta$ ,  $\bar{w} = |w| e^{i\theta}$ , then in our coordinate system, the uniform velocities at up- and downstream infinities are  $U e^{i\alpha}$  and  $V e^{i\alpha}$  respectively.

The boundary conditions for the problem are:

$$\begin{aligned}\theta &= \alpha, & \text{on the channel walls} \\ \theta &= 0, & \text{on the plate from D to B} \\ \theta &= \pi, & \text{on the plate from D to A} \\ |w| &= V, & \text{on the cavity walls.}\end{aligned}$$

The force coefficients at the choking condition can be obtained from momentum consideration in terms of the channel width, the angle of attack and the critical cavitation number;

$$\rho V^2 (h_1 + h_2) - \rho U^2 W = (p_\infty - p_c) W - F_D \quad (2)$$

where  $F_D$  is the drag, by conservation of volume,  $V(h_1 + h_2) = WU$  and by definition  $\sigma^* = (p_\infty - p_c) / \frac{1}{2} \rho U^2$ . Substituting

$$F_D = (p_\infty - p_c) W + \rho U^2 W - \rho V U W \quad (3)$$

---

\* The subscript is dropped since the cavitation number we refer to from now on is always the choked one.

and the drag coefficient is

$$C_D = \frac{2F_D}{\rho U^2 A^+} = 2W \left[ \left(1 + \frac{\sigma}{2}\right) - \sqrt{1 + \sigma} \right]. \quad (4)$$

$A^+$ , the area per unit span, is equal to one for a plate of unit length. The lift coefficient is

$$C_L = C_D \cot \alpha. \quad (5)$$

### Theory

Assuming the flow to be irrotational, there exists a complex potential  $f = \varphi + i\psi$ . The flow field in the  $f$ -plane is shown in Fig. 2. The two channel walls are represented by the streamlines  $\psi_1$  and  $-\psi_2$  while the dividing streamline coincides with the negative  $\varphi$ -axis. The stagnation point  $D$  is chosen as the origin and the cut along the positive  $\varphi$ -axis represents the two branches of the streamline split at  $D$ . The leading and trailing edges of the plate are located somewhere on the upper and lower branches respectively. With reference to Fig. 1, the values of  $\psi_1$  and  $\psi_2$  are given as

$$\begin{aligned} \psi_1 &= UH_1 = Vh_1 \\ \psi_2 &= UH_2 = Vh_2. \end{aligned} \quad (6)$$

We proceed to solve the problem by introducing a new variable  $\Omega$ , defined by

$$\begin{aligned} \Omega &= \log \frac{V}{w} = \tau + i\theta \\ \tau &= \log \frac{V}{|w|}, \quad \theta = -\arg w. \end{aligned} \quad (7)$$

The choice of using  $\Omega$  as the dependent variable for the problem is suggested by the existing boundary conditions.

The flow fields in the  $f$  and the  $\Omega$ -planes are to be connected through a parametric variable  $\zeta = \xi + i\eta$ . Consider the transformation

$$\frac{df}{d\zeta} = \frac{C}{(\zeta - k_0)(\zeta - k_1)(\zeta - k_2)} \quad (8a)$$

or

$$f(\zeta) = \frac{1}{\pi} [(h_1 + h_2) \log(\zeta - k_0) - h_1 \log(\zeta - k_1) - h_2 \log(\zeta - k_2)]. \quad (8b)$$

The flow in the  $f$ -plane is mapped into the upper half  $\zeta$ -plane with the boundaries on the real  $\zeta$  or  $\xi$ -axis as shown in Fig. 3. The upstream I behaves like a source at  $\xi = k_0$  while the downstreams J and K behave like sinks at  $\xi = k_1$  and  $k_2$  respectively. The net strength of these singularities is certainly zero. The jump conditions on the  $f$ -plane further furnish the relations;

$$h_1 = \frac{-\pi C}{V} \frac{1}{(k_2 - k_1)(k_0 - k_1)} \quad (9)$$

and

$$h_2 = \frac{-\pi C}{V} \frac{1}{(k_2 - k_1)(k_2 - k_0)} \quad (10)$$

Combining Eqs. (9) and (10) yields the ratio

$$\frac{h_1}{h_2} = \frac{k_2 - k_0}{k_0 - k_1} \quad (11)$$

The constant  $C$  is a scale factor to be determined later in the theory.

$\Omega$  has the following values along the  $\xi$ -axis and  $\eta = 0_+$ .

$$\begin{aligned} \text{Im } \Omega &= \pi, & \xi < -1 \\ \text{Im } \Omega &= 0, & \xi > 1 \\ \text{Re } \Omega &= 0, & -1 < \xi < k_1, \quad k_2 < \xi < 1 \\ \text{Im } \Omega &= \alpha, & k_1 < \xi < k_2. \end{aligned} \quad (12)$$

We further define

$$\Omega = \Omega_0 + \Omega_1, \quad (13)$$

where  $\Omega_0$  is associated with the unbounded fluid.  $\Omega$  is split up in this way to make the solution readily obtainable. The term  $\Omega_1$ , which represents the effect of the walls, is added to the unbounded fluid transcendently to maintain the total exact solution. When the channel width-chord ratio is very large,  $\Omega_1$  then can be considered merely as a perturbation of the unbounded flow.

With reference to Figures 4a and 4b,  $\Omega_0$  has the form

$$\Omega_0 = \cosh^{-1} \zeta = \log (\zeta + \sqrt{\zeta^2 - 1}). \quad (14)$$

Along the  $\xi$ -axis,

$$\begin{aligned} \operatorname{Im} \Omega_0 &= \pi, & \xi < -1 \\ \operatorname{Im} \Omega_0 &= 0, & \xi > 1 \\ \operatorname{Re} \Omega_0 &= 0, & -1 < \xi < 1. \end{aligned} \quad (15)$$

For  $|\xi| < 1$ ,  $\Omega_0$  is given by

$$\operatorname{Im} \Omega_0 = \beta(\xi) = \arctan (\sqrt{1 - \xi^2} / \xi). \quad (16)$$

The remaining part,  $\Omega_1$  which is caused by the presence of the channel walls, then takes the boundary values;

$$\begin{aligned} \operatorname{Im} \Omega_1 &= 0, & \xi < -1 \\ \operatorname{Im} \Omega_1 &= 0, & \xi > 1 \\ \operatorname{Re} \Omega_1 &= 0, & -1 < \xi < k_1, \quad k_2 < \xi < 1 \\ \operatorname{Im} \Omega_1 &= \alpha - \beta(\xi), & k_1 < \xi < k_2. \end{aligned} \quad (17)$$

The boundary condition for  $\Omega_1$  on the  $\xi$ -axis is shown in Fig. 5. Three branch cuts appear on the  $\xi$ -axis; these are from  $\xi = -\infty$  to  $\xi = -1$ , from  $\xi = 1$  to  $\xi = +\infty$  and from  $\xi = k_1$  to  $\xi = k_2$ . The first two cuts represent the plate and the last one the channel walls in the  $z$ -plane.

We now have a boundary value problem involving the unknown function,  $\Omega_1(\zeta)$ , which can be formulated and solved as a Hilbert problem. By analytic continuation

$$\Omega_1(\bar{\zeta}) = -\bar{\Omega}_1(\zeta). \quad (18)$$

The region is extended to the lower half  $\zeta$ -plane with the  $\operatorname{Re} \Omega_1$  odd and the  $\operatorname{Im} \Omega_1$  even with respect to the  $\xi$ -axis. We now introduce the auxiliary function

$$H(\zeta) = \frac{1}{\sqrt{(\zeta - k_1)(\zeta - k_2)(\zeta^2 - 1)}}, \quad (19)$$

which has the following properties;

i)  $H(\zeta)$  has the proper branch cuts ( $\zeta = -1, k_1, k_2$ , and  $+1$  are branch points).

ii) On the  $\text{Re } \zeta$  axis:

$$\begin{aligned} \text{Im } H &= 0, & -\infty < \xi < -1 \\ \text{Re } H &= 0, & -1 < \xi < k_1 \\ \text{Re } H &= -\frac{1}{\sqrt{(\xi - k_1)(k_2 - \xi)(1 - \xi^2)}}, & \text{Im } H &= 0, \quad k_1 < \xi < k_2 \\ \text{Re } H &= 0, & k_2 < \xi < 1 \\ \text{Im } H &= 0, & 1 < \xi < \infty \end{aligned}$$

A new function

$$G(\zeta) = \Omega_1(\zeta) H(\zeta)$$

is then formed which has on the  $\text{Re } \zeta$  axis;

$$\begin{aligned} \text{Im } G &= 0, & -\infty < \xi < k_1 \\ \text{Im } G &= -\frac{\alpha - \beta(\xi)}{\sqrt{(\xi - k_1)(k_2 - \xi)(1 - \xi^2)}}, & k_1 < \xi < k_2 \\ \text{Im } G &= 0, & k_2 < \xi < +\infty \end{aligned}$$

With the aid of Plemelj's formula<sup>(7)</sup>, the solution of the Hilbert problem is given immediately by

$$\Omega_1(\zeta) = -\frac{1}{\pi} \sqrt{(\zeta - k_1)(\zeta - k_2)(\zeta^2 - 1)} \int_{k_1}^{k_2} \frac{[\alpha - \beta(t)] dt}{(t - \zeta) \sqrt{(t - k_1)(k_2 - t)(1 - t^2)}} \quad (20)$$

However, the constants  $k_1$  and  $k_2$  cannot be arbitrarily chosen for a fixed  $\alpha$  because of a physical condition that must be imposed on the solution. Specifically, the solution  $\Omega$  must behave locally like a stagnation flow at the stagnation point. In the  $\zeta$ -plane, the stagnation point corresponds to  $\zeta = \infty$ . The local stagnation flow can be shown to behave like  $\log \zeta$  as  $\zeta$  approaches infinity; this behavior is already incorporated into the function  $\Omega_0$ . We require, therefore that  $\Omega_1$  be finite at infinity. If Eq. (20) is expanded in inverse powers of  $\zeta$ , this condition is seen to be given by the requirement that



$$\int_{k_1}^{k_2} \frac{a - \beta(t)}{\sqrt{(t-k_1)(k_2-t)(1-t^2)}} dt = 0. \quad (21)$$

Thus for a given value of  $a$ , Eq. (21) determines the relation between  $k_1$  and  $k_2$ .

We are now able to determine  $\sigma$  from  $\Omega_1$  in Eq. (20). At upstream infinity in the physical plane,  $|w| = U$  and  $\zeta = k_0$ .

$$\Omega_1 = \tau_1 = \log \frac{V}{U} = \frac{1}{\pi} \sqrt{(k_2 - k_0)(k_0 - k_1)(1 - k_0^2)} \int_{k_1}^{k_2} \frac{[a - \beta(t)] dt}{(t - k_0) \sqrt{(t - k_1)(k_2 - t)(1 - t^2)}}. \quad (22)$$

From our previous discussion,  $\sigma = V^2/U^2 - 1$ , therefore Eq. (22) enables us to calculate  $\sigma$  when the integral on the right hand side is evaluated.

In order to complete the solution, we shall relate the geometry of the flow to the undetermined constants. Utilizing the definition of the complex velocity, we have the relation

$$dz = \frac{1}{w} df = \frac{1}{w} \frac{df}{d\zeta} d\zeta = \frac{1}{V} e^{\Omega(\zeta)} \frac{df}{d\zeta} d\zeta. \quad (23)$$

With the aid of Eqs. (8a), (13) and (14) and upon integration,

$$\int dz = \frac{C}{V} \int \frac{\zeta + \sqrt{\zeta^2 - 1}}{(\zeta - k_0)(\zeta - k_1)(\zeta - k_2)} e^{\Omega_1(\zeta)} d\zeta. \quad (24)$$

When we apply Eq. (24) along the plate from A to B, the normalized chord is obtained;

$$z_B - z_A = 1 = \frac{C}{V} \left[ \int_{\infty}^1 \frac{\xi + \sqrt{\xi^2 - 1}}{(\xi - k_0)(\xi - k_1)(\xi - k_2)} e^{\Omega_1(\xi)} d\xi - \int_{-\infty}^{-1} \frac{\xi - \sqrt{\xi^2 - 1}}{(\xi - k_0)(\xi - k_1)(\xi - k_2)} e^{\Omega_1(\xi)} d\xi \right]. \quad (25)$$

The first integral on the right hand side represents the distance from the stagnation point to the trailing edge, we therefore find the location of the stagnation point.

$H_A$ , the height of A below the upper channel wall can be determined in a similar way. With reference again to Fig. 1,

$$\begin{aligned}
H_A &= h_1 + \text{Im} \left[ e^{-i\alpha} (z_J - z_A) \right] \\
&= h_1 + \frac{C}{V} \text{Im} \left[ e^{-i\alpha} \int_{-1}^{k_1} \frac{e^{i\beta(\xi)} e^{\Omega_1(\xi)}}{(\xi - k_0)(\xi - k_1)(\xi - k_2)} d\xi \right] \\
\text{or} \\
&= h_1 + \frac{C}{V} \int_{-1}^{k_1} \frac{\sin(\theta_1 + \beta - \alpha)}{(\xi - k_0)(\xi - k_1)(\xi - k_2)} d\xi,
\end{aligned} \tag{26}$$

since  $\Omega_1$  is purely imaginary and equal to  $i\theta_1$  in the interval  $-1 \leq \xi \leq k_1$ .

The channel width  $W$  is expressed through continuity as

$$W = (h_1 + h_2) \frac{V}{U} = \frac{(h_1 + h_2)}{\sqrt{1 + \sigma}}. \tag{27}$$

#### Final Results.

We have applied the theory to calculate the case of a flat plate positioned mid-channel for various values of  $\alpha$  and  $W$ . The range in  $\alpha$  is from  $5^\circ$  to  $90^\circ$  and in  $W$  from 3 chords to 20 chords. We also obtained results for two off-center positions of the plate,  $H_A = 1.0$  and  $4.0$  for  $W = 5$  chords and values of  $\alpha$  up to  $30^\circ$ .

The lift coefficient, drag coefficient and choking cavitation number are plotted versus  $\alpha$  for  $W = 5$  chords and the plate in mid-channel in Fig. 6. The dash-dot curve in Fig. 6 is the lift coefficient given by Wu's unbounded fluid theory<sup>(1)</sup>.

In Fig. 7, we show the enlarged portion of Fig. 6 for  $\alpha \leq 30^\circ$  with experimental values from Wade<sup>(8)</sup> corresponding to the choking  $\sigma$  determined by the present theory. Wade's experiment was performed with  $W \approx 5$  and the experimental cavitation numbers were obtained from measured cavity pressure. Since it is difficult to operate the tunnel near choking condition, Wade was not able to obtain data at such low cavitation numbers: Therefore, we show values extrapolated from his data curves. One notices that all points are enveloped by the two theoretical curves.

Cohen, Sutherland and Tu<sup>(5)</sup> have worked out a linearized theory for a flat plate at small angles of attack and calculated  $\sigma$  for mid-channel position. However, their definition of mid-channel is different from ours as we define mid-channel when the center of the plate lies on the centerline while they locate the leading edge of the plate on the centerline. As a result, it is not possible to make a direct comparison between the two theories. For very small angles of attack, however, the discrepancy caused by the difference in definition becomes small and for  $\alpha = 6^\circ$ ,  $W = 5$ , the present theory gives  $\sigma = 0.133$ ,  $C_L = 0.198$  for  $H_A/(W-H_A) = 0.959$  and their theory gives  $\sigma \approx 0.13$  and  $C_L \approx 0.22$  for  $H_A/(W-H_A) = 1$ . The values of their calculations are read from Fig. 10 of Ref. 3, hence are only approximate.

Figure 8 shows the effect of plate position for  $W = 5$  chords. In this figure  $C_L$ ,  $C_D$  and  $\sigma$  are plotted versus  $\alpha$  for  $\alpha \leq 30^\circ$  and two values of  $H_A$ . The dashed curves are  $H_A = 1.0$  and the solid ones are  $H_A = 4.0$ . As would be expected  $C_L$ ,  $C_D$  and  $\sigma$  all increase as the plate is lowered in the channel.

We show  $C_L$  and  $\sigma$  versus  $\alpha$  for  $W = 8$  with experimental values from Parkin<sup>(9)</sup> in Fig. 9. Again the experimental cavitation numbers were obtained from measured cavity pressure, however, in this case only the data for  $\alpha = 8^\circ$  and  $10^\circ$  were obtained from extrapolated curves.

Figures 10a and b show drag coefficient,  $C_D$ , and choking cavitation number,  $\sigma$ , versus channel width,  $W$ , for a flat plate located mid-channel. The range in angle of attack is  $5^\circ$  to  $90^\circ$  and in  $W$  from 3 to 20 chords.  $C_L$  may easily be obtained from Fig. 10a and Eq. (5) and therefore is not presented here.

In order to show the effect of the channel walls, we have plotted  $RC_D$ , the ratio of  $C_D$  bounded to  $C_D$  unbounded<sup>(1)</sup>, ( $RC_N = RC_L = RC_D$ ) versus the channel width  $W$  in Fig. 11. The curves are for the same values of  $\alpha$  and  $W$  as Figs. 10a and b except that for  $\alpha = 90^\circ$   $RC_D$  is shown for  $W$  as low as 1.224. As would be expected when  $W = 20$  there is very little wall effect and as the channel becomes smaller the ratio drops until the walls approach the plate where the ratio increases. This effect is shown for  $\beta = 90^\circ$  where the ratio tends to infinity at  $W = 1$ .

The curve of  $RC_D$  for each  $\alpha$  will have a similar asymptote at  $W = \sin \alpha$ .

In Fig. 12, we have shown the distance of the stagnation point from the leading edge as a function of  $\alpha$ . At  $\alpha = 15^\circ$ , it is already difficult to tell the difference between the two points and at  $\alpha = \frac{\pi}{2}$  the stagnation point is at mid-plate as one would expect.

#### ACKNOWLEDGMENT

This work is supported by the U. S. Office of Naval Research under Contract Nonr-220(41) at the California Institute of Technology. The authors also wish to express their sincere thanks to Professor T. Y. Wu for his suggestions and guidance in this problem, to Dr. D. P. Wang for the many helpful discussions they had, and to Miss C. Lin for the graphical works.

## REFERENCES

1. Wu, T. Y., "A wake model for free-streamline flow theory. Part I. Fully and partially developed wake flows and cavity flows past an oblique flat plate", Journal of Fluid Mechanics, Vol. 13 part 2, pp. 161-181, 1962.
2. Wu, T. Y. and Wang, D. P., "A wake model for free-streamline flow theory, Part II, Cavity flows past obstacles of arbitrary Profile", California Institute of Technology, Hydrodynamics Laboratory Report No. 97.4, May 1963.
3. Cohen, H. and DiPrima, R. C., "Wall effects in cavitating flows", pp. 367-390, Aug. 25--29, 1958.
4. Birkhoff, G., Plesset, M. and Simmons, N., "Wall effects in cavity flow I", Quarterly of Applied Mathematics, Vol. VIII, No. 2, July 1950.
5. Cohen, H., Sutherland, C. C. and Tu, Yih-O, "Wall effects in cavitating hydrofoil flow", Journal of Ship Research, 3, (1957), pp. 31-40.
6. Gurevich, M. I., "Symmetrical cavitation flow around a flat plate situated between parallel walls", Bull. of Acad. of Sci, of USSR, No. 4(1946).
7. Mikhlin, S. G., "Integral equations", Pergamon Press, 1957.
8. Wade, R. B., "Water tunnel observations on the flow past a plano-convex hydrofoil", California Institute of Technology, Hydrodynamics Laboratory Report No. E-79.6, Feb. 1964.
9. Parkin, B. R., "Experiments on circular arc and flat plate hydrofoils in non-cavitating and full cavity flows", California Institute of Technology, Hydrodynamics Laboratory Report No. 47.6, Feb. 1956.

## APPENDIX

### Procedures for numerical computations

In a direct problem one would specify the channel width,  $W$ , and the location of the plate (of chord unity),  $H_A$ , for a given angle of attack, then calculate  $\sigma$ ,  $h_1$ ,  $h_2$  and the force coefficients. However, in view of the form of our solution it is necessary to do the inverse problem of choosing the transformation parameters  $k_2$ ,  $k_1$ , and  $k_0$  (the downstream conditions,  $h_1$  and  $h_2$ , when the flow is choked) and calculating  $W$  and  $H_A$ . The values of  $h_1$  and  $h_2$  are related to the  $k$ 's through the transformations in Eqs. (8a), (8b) and the jump conditions in Eqs. (9) and (10). The choice of  $k_2$  defines the geometry so that the scaling factor,  $C$ , or more precisely, the ratio  $V/C$  is determined from Eq. (25).

Given a value of  $k_2$ ,  $k_1$  is easily determined by iteration of the integral condition of Eq. (21). The integral in this equation cannot be numerically integrated in its present form so we divide it into two integrals

$$\int_{k_1}^{k_2} \frac{a - \beta(t)}{\sqrt{(t-k_1)(k_2-t)(1-t^2)}} dt = \int_{k_1}^{\frac{k_1+k_2}{2}} \frac{a - \beta(t)}{\sqrt{(t-k_1)(k_2-t)(1-t^2)}} dt + \int_{\frac{k_1+k_2}{2}}^{k_2} \frac{a - \beta(t)}{\sqrt{(t-k_1)(k_2-t)(1-t^2)}} dt; \quad (A-1)$$

make the transformations

$$p = x^2 + k_1 \quad \text{in the first integral,}$$

$$s = k_2 - x^2 \quad \text{in the second integral,}$$

and

$$x_0^2 = \frac{1}{2}(k_2 - k_1)$$

and Eq. (21) becomes

$$\int_0^{x_0} \frac{a - \beta(p)}{p^2 \sqrt{2x_0^2 - x^2}} dx + \int_0^{x_0} \frac{a - \beta(s)}{s^2 \sqrt{2x_0^2 - x^2}} dx = 0. \quad (A-2)$$

This integral iteration presents no problem since all calculations are performed on a high speed digital computer (IBM 7094). We now can calculate the remaining transformation parameter,  $k_0$ , from the specified ratio  $h_2/h_1$  and Eq. (11).

To aid in the trial and error solution of this problem the behavior of  $k_2$  and  $k_1$  for the plate in mid-channel are shown in Fig. A-1 and for the off center positions in Fig. A-2. The remaining parameter to be guessed is  $h_2/h_1$  which may be approximated by  $(W-H_A \sin \alpha)/H_A$ . For the mid-channel case this quantity is roughly unity.

The choking cavitation number,  $\sigma$ , the channel width,  $W$ , the drag coefficient,  $C_D$ , and the lift coefficient,  $C_L$ , are readily determined from Eqs. (22), (27), (4) and (5) respectively. The integral in Eq. (22) is treated in the same way as Eq. (21).

To determine  $H_A$  we must first evaluate the ratio  $V/C$ . From Eq. (25)

$$\frac{V}{C} = - \int_1^{\infty} \frac{\xi + \sqrt{\xi^2 - 1}}{(\xi - k_0)(\xi - k_1)(\xi - k_2)} e^{\Omega_1(\xi)} d\xi - \int_1^{\infty} \frac{\xi + \sqrt{\xi^2 - 1}}{(\xi + k_0)(\xi + k_1)(\xi + k_2)} e^{\Omega_1'(\xi)} d\xi, \quad (A-3)$$

where  $\Omega_1(\xi)$  is given in Eq. (20) and

$$\Omega_1'(\xi) = - \frac{1}{\pi} \sqrt{(\xi + k_1)(\xi + k_2)(\xi^2 - 1)} \int_{k_1}^{k_2} \frac{\alpha - \beta(t)}{(t + \xi)\sqrt{(t - k_1)(k_2 - t)(1 - t^2)}} dt. \quad (A-4)$$

For numerical integration, it is more convenient to introduce the new integration variable  $\tau = \xi^{-1}$ . The first integral on the right hand side of Eq. (A-3) now may be written

$$\int_1^{\infty} \frac{\xi + \sqrt{\xi^2 - 1}}{(\xi - k_0)(\xi - k_1)(\xi - k_2)} e^{\Omega_1(\xi)} d\xi = \int_0^{\tau_0} \frac{1 + \sqrt{1 - \tau^2}}{(1 - k_0 \tau)(1 - k_1 \tau)(1 - k_2 \tau)} e^{\Omega_1^\dagger} d\tau + \int_{\tau_0}^1 \frac{1 + \sqrt{1 - \tau^2}}{(1 - k_0 \tau)(1 - k_1 \tau)(1 - k_2 \tau)} e^{\Omega_1^*} d\tau, \quad (A-5)$$

and the second integral

$$\int_1^{\infty} \frac{\xi + \sqrt{\xi^2 - 1}}{(\xi + k_0)(\xi + k_1)(\xi + k_2)} e^{\Omega_1'(\xi)} d\xi =$$

$$\int_0^{\tau_0} \frac{1 + \sqrt{1 - \tau^2}}{(1 + k_0\tau)(1 + k_1\tau)(1 + k_2\tau)} e^{\Omega_1'^+} d\tau + \int_{\tau_0}^1 \frac{1 + \sqrt{1 - \tau^2}}{(1 + k_0\tau)(1 + k_1\tau)(1 + k_2\tau)} e^{\Omega_1'^*} d\tau, \quad (A-6)$$

where

$$\Omega_1'^+ = \frac{1}{\pi} \sqrt{(1 - k_1\tau)(1 - k_2\tau)(1 - \tau^2)} [g_1 + \tau g_2 + \tau^2 g_3 + \dots + \tau^6 g_7], \quad (A-7)$$

$$\Omega_1'^+ = \frac{1}{\pi} \sqrt{(1 + k_1\tau)(1 + k_2\tau)(1 - \tau^2)} [g_1 - \tau g_2 + \tau^2 g_3 - \dots + \tau^6 g_7], \quad (A-8)$$

$$\Omega_1'^* = \frac{1}{\pi\tau} \sqrt{(1 - k_1\tau)(1 - k_2\tau)(1 - \tau^2)} \int_{k_1}^{k_2} \frac{a - \beta(t)}{(1 - t\tau)\sqrt{(t - k_1)(k_2 - t)(1 - t^2)}} dt, \quad (A-9)$$

$$\Omega_1'^* = -\frac{1}{\pi\tau} \sqrt{(1 + k_1\tau)(1 + k_2\tau)(1 - \tau^2)} \int_{k_1}^{k_2} \frac{a - \beta(t)}{(1 + t\tau)\sqrt{(t - k_1)(k_2 - t)(1 - t^2)}} dt, \quad (A-10)$$

and

$$g_n = \int_{k_1}^{k_2} \frac{t^n [a - \beta(t)] dt}{\sqrt{(t - k_1)(k_2 - t)(1 - t^2)}}. \quad (A-11)$$

$\Omega_1^+$  and  $\Omega_1'^+$  are obtained from the power series expansion of  $\tau$  and therefore are suitable for the calculation of small values of  $\tau$  or large values of  $\xi$ . For a properly chosen  $\tau_0$ , say  $\tau_0 = 0.1$ , a truncated series of seven terms is sufficient to give  $\Omega_1^+(\tau_0)$  identical to  $\Omega_1'^*(\tau_0)$  to five significant figures.

The remaining quantity to be evaluated is the integral in Eq. (26)



$$\int_1^k \frac{\sin(\theta_1 + \beta - \alpha)}{(\xi - k_0)(\xi - k_1)(\xi - k_2)} d\xi.$$

Some analysis is needed before a straightforward numerical integration can be performed. One notices that the denominator of the integrand has a factor  $(\xi - k_1)$  which causes the integral to be logarithmically singular unless the numerator also vanishes at the upper limit. It is therefore necessary to examine the behavior of the numerator as  $\xi$  approaches  $k_1$ . Let us study the behavior of

$$\theta_1 = \frac{1}{\pi} \sqrt{(k_1 - \xi)(k_2 - \xi)(1 - \xi^2)} \int_{k_1}^k \frac{\alpha - \beta(t)}{(t - \xi)\sqrt{(t - k_1)(k_2 - t)(1 - t^2)}} dt \quad (\text{A-12})$$

as  $\xi$  approaches  $k_1$ . We denote the regular part of the integrand in the neighborhood of  $t = k_1$  as

$$F(t) = \frac{\alpha - \beta(t)}{\sqrt{(k_2 - t)(1 - t^2)}}. \quad (\text{A-13})$$

$F(t)$  has the Taylor expansion

$$F(t) = F(k_1) + F'(k_1)(t - k_1) + \frac{F''(k_1)}{2} (t - k_1)^2 + \dots$$

where the coefficients  $F(k_1)$ ,  $F'(k_1)$  etc. are finite numbers which can be evaluated without any difficulty. If we now subtract from  $F(t)$  the first terms of its Taylor expansion then add them on later, the integral in  $\theta_1$  can be written

$$\begin{aligned} & \int_{k_1}^k \frac{[\alpha - \beta(t)] dt}{(t - \xi)\sqrt{(t - k_1)(k_2 - t)(1 - t^2)}} = \\ & \int_{k_1}^k \frac{dt}{(t - \xi)\sqrt{t - k_1}} \left[ F(t) - F(k_1) - F'(k_1)(t - k_1) - \frac{F''(k_1)}{2} (t - k_1)^2 \right] \\ & + F(k_1) \int_{k_1}^k \frac{(t - k_1)^{-\frac{1}{2}}}{t - \xi} dt + F'(k_1) \int_{k_1}^k \frac{(t - k_1)^{\frac{1}{2}}}{t - \xi} dt + \frac{F''(k_1)}{2} \int_{k_1}^k \frac{(t - k_1)^{\frac{3}{2}}}{t - \xi} dt. \end{aligned} \quad (\text{A-14})$$

The integrand of the first integral of Eq. (A-14) is finite and tends to zero as  $t$  approaches  $k_1$  because the terms in the bracket are of the order  $(t-k_1)^3$ . The remaining integrals of Eq. (A-14) are integrated in closed form:

$$\int_{k_1}^k \frac{1}{t-\xi} \frac{dt}{\sqrt{t-k_1}} = \frac{2}{\sqrt{k_1-\xi}} \left[ \frac{\pi}{2} - \tan^{-1} \sqrt{\frac{k_1-\xi}{k_2-k_1}} \right]$$

$$\int_{k_1}^k \frac{\sqrt{t-k_1}}{t-\xi} dt = 2\sqrt{k_2-k_1} - 2\sqrt{k_1-\xi} \left[ \frac{\pi}{2} - \tan^{-1} \sqrt{\frac{k_1-\xi}{k_2-k_1}} \right]$$

$$\int_{k_1}^k \frac{(t-k_1)^{\frac{3}{2}}}{t-\xi} dt = \frac{2}{3} (k_2-k_1)^{\frac{3}{2}} - 2(k_2-k_1)\sqrt{k_1-\xi} + 2(k_1-\xi)^{\frac{3}{2}} \left[ \frac{\pi}{2} - \tan^{-1} \sqrt{\frac{k_1-\xi}{k_2-k_1}} \right].$$

From Eqs. (A-13) and (A-14) it can be shown that in the neighborhood of  $\xi = k_1$ ,  $\theta_1$  has the asymptotic expression

$$\theta_1 = \alpha - \beta + M\sqrt{k_1-\xi} + O(k_1-\xi)$$

where

$$M = \frac{\sqrt{(k_2-k_1)(1-k_1^2)}}{\pi} \int_{k_1}^k \frac{dt}{(t-k_1)^{\frac{3}{2}}} \left[ F(t) - F(k_1) - F'(k_1)(t-k_1) - \frac{F''(k_1)}{2}(t-k_1)^2 \right]$$

$$= \frac{2}{\pi} \frac{\alpha - \beta(k_1)}{\sqrt{k_2-k_1}} + \frac{2F'(k_1)}{\pi} \sqrt{1-k_1^2} (k_2-k_1) + \frac{F''(k_1)}{3\pi} \sqrt{1-k_1^2} (k_2-k_1)^2. \quad (A-15)$$

In our final form for numerical computation, the range of integration of the integral in Eq. (26) is split into two intervals;

$$\int_{-1}^{k_1} \frac{\sin(\theta_1 + \beta - \alpha)}{(\xi - k_0)(\xi - k_1)(\xi - k_2)} d\xi = \int_{-1}^{k_1 - \epsilon} \frac{\sin(\theta_1 + \beta - \alpha)}{(\xi - k_0)(\xi - k_1)(\xi - k_2)} d\xi + \int_{k_1 - \epsilon}^{k_1} \frac{(\theta_1 + \beta - \alpha) d\xi}{(\xi - k_0)(\xi - k_1)(\xi - k_2)}, \quad (\text{A-16})$$

where  $\epsilon$ , small and positive, is chosen so that at  $\xi = k_1 - \epsilon$ ,  $\sin(\theta_1 + \beta - \alpha)$  can be safely approximated by  $\theta_1 + \beta - \alpha$ . If we replace  $\theta_1$ , in the second integral of Eq. (A-16) by its asymptotic expression, Eq. (26) becomes

$$H_A = h_1 + \frac{C}{V} \left[ \int_{-1}^{k_1 - \epsilon} \frac{\sin(\theta_1 + \beta - \alpha)}{(\xi - k_0)(\xi - k_1)(\xi - k_2)} d\xi - 2M \int_0^{\sqrt{\epsilon}} \frac{d\lambda}{(k_0 - \xi)(k_2 - \xi)} \right], \quad (\text{A-17})$$

where

$$\lambda^2 = k_1 - \xi$$

The integrals in Eq. (A-17) can be easily evaluated since their integrands are regular everywhere.

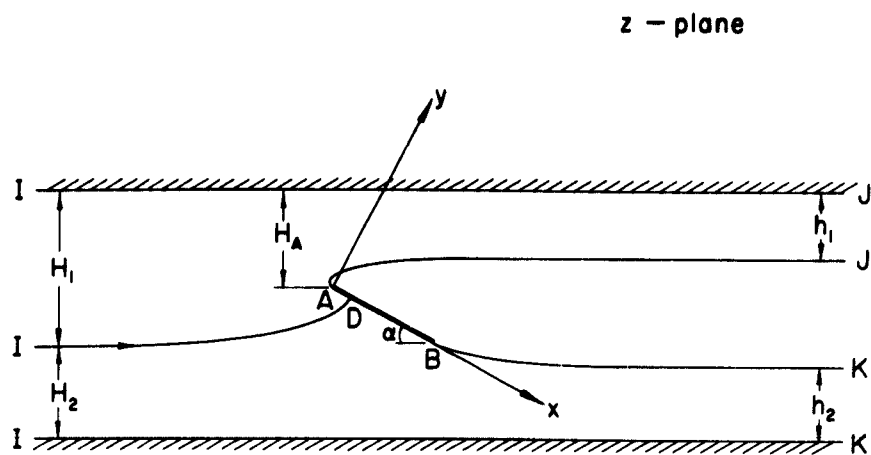


Fig. 1 Sketch showing a flat plate with an infinite cavity in a water tunnel.

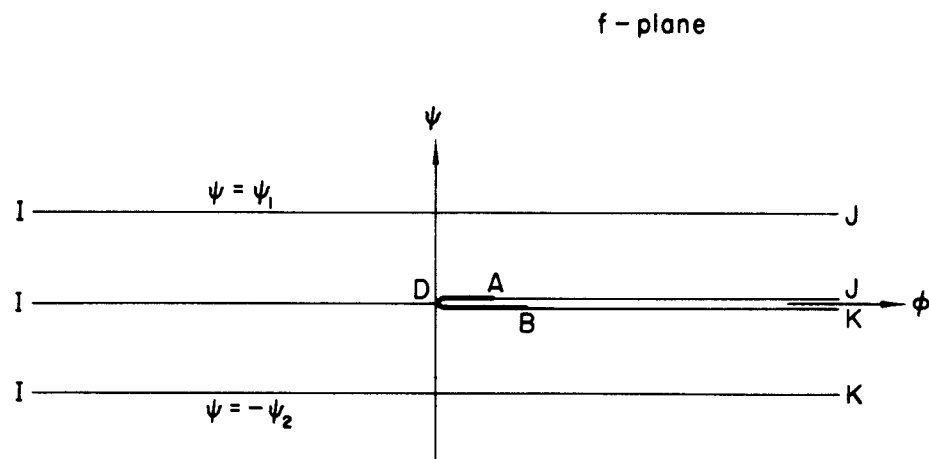


Fig. 2 The complex potential plane of the flow.

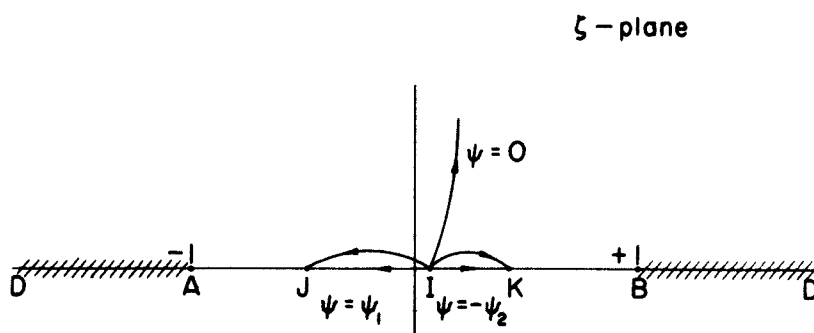


Fig. 3 The parametric  $\zeta$ -plane.

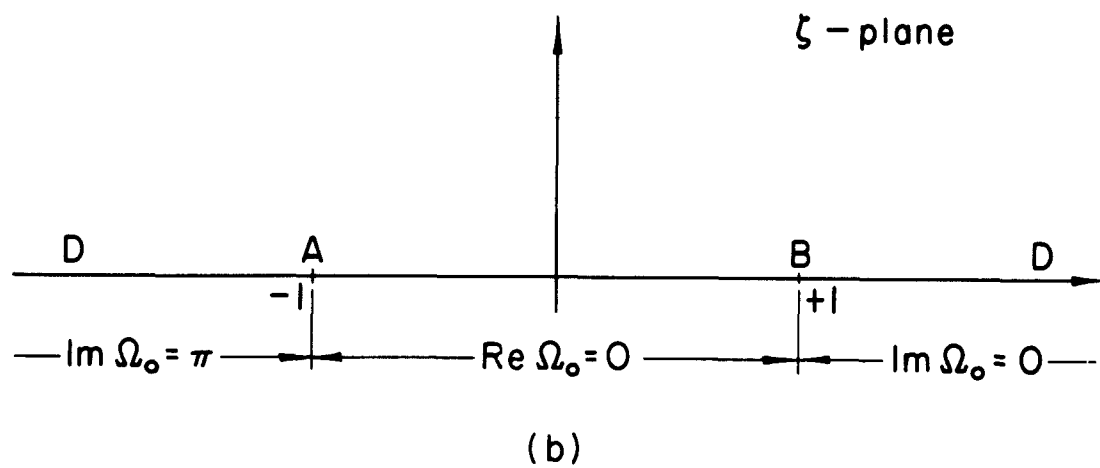
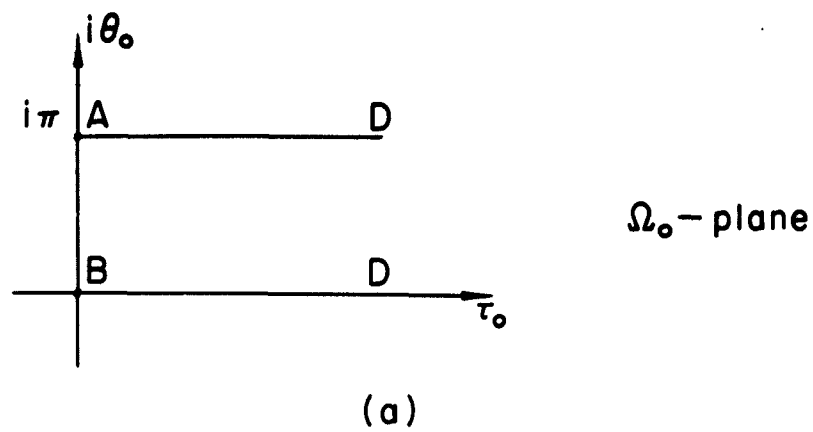


Fig. 4 The  $\Omega_0$ - and  $\zeta$ -planes.  $\Omega_0 = \cosh^{-1} \zeta = \log(\zeta + \sqrt{\zeta^2 - 1})$ .

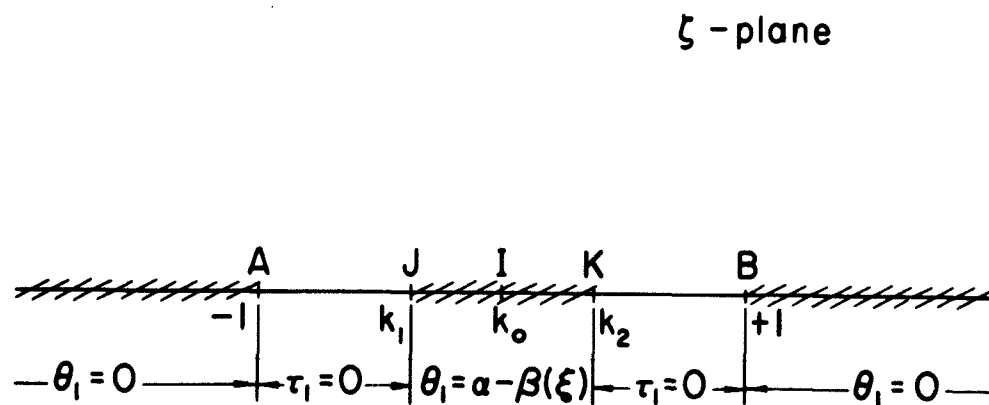


Fig. 5 Boundary values of  $\Omega_1$  on  $\text{Re } \zeta$ -axis.

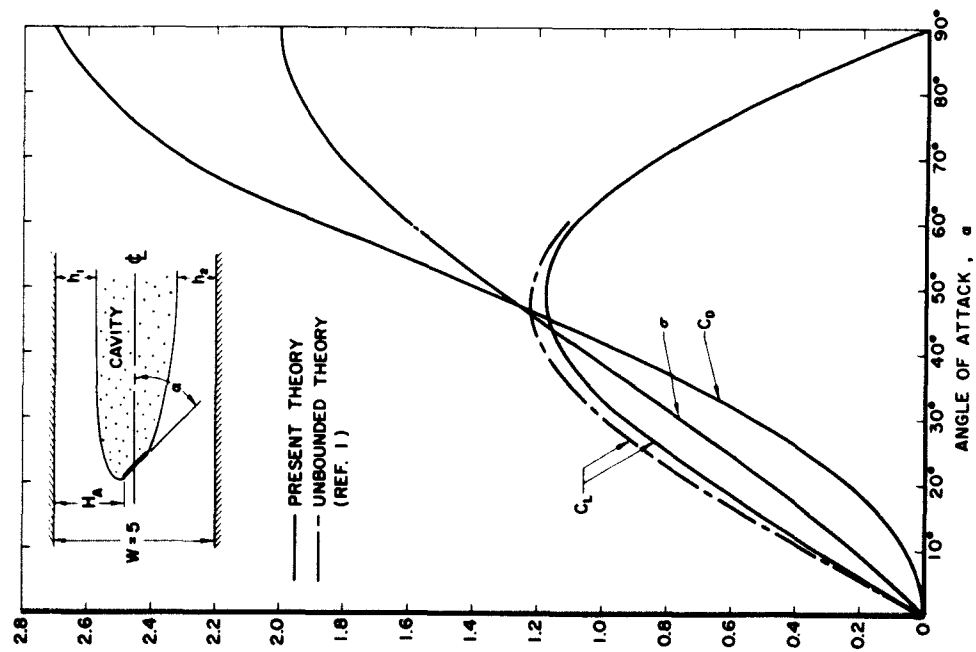


Fig. 6 The dependence of  $C_L$ ,  $C_D$  and  $\sigma$  on the angle of attack,  $\alpha$ , for a flat plate located midway in a channel of width  $W = 5$ .

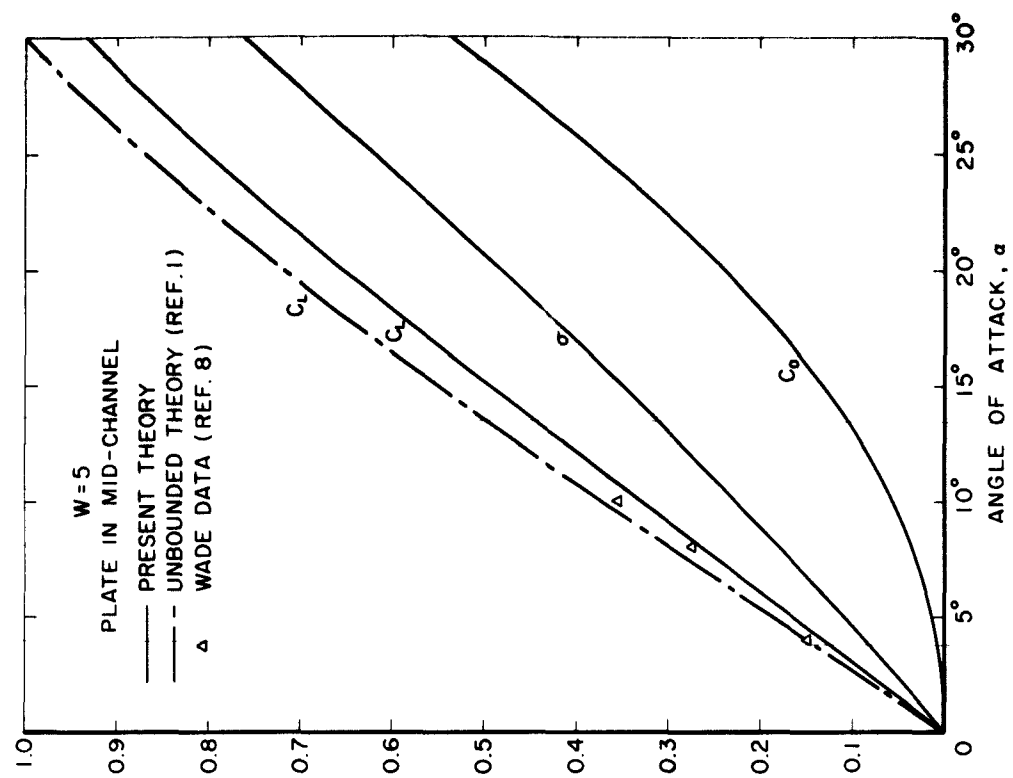


Fig. 7 Enlarged section of Fig. 6 for small angles of attack with experimental data extrapolated from Wade's data curves.

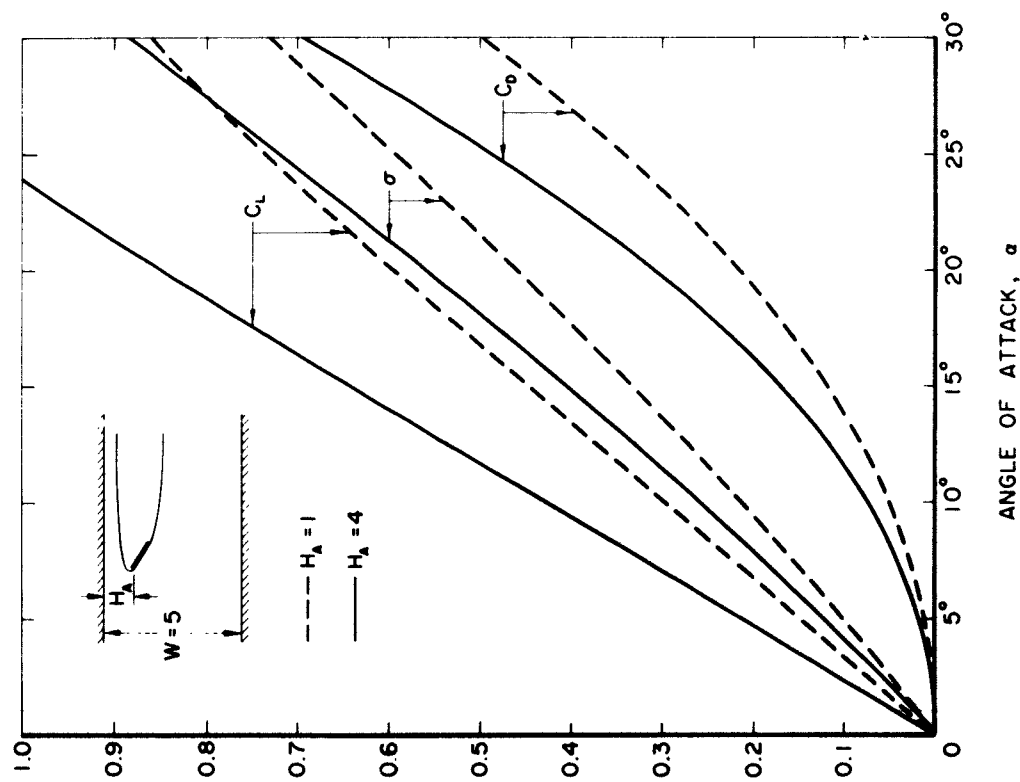


Fig. 8 The effect of angle of attack on  $C_L$ ,  $C_D$  and  $\sigma$  for a flat plate located in two off-center positions in a channel of  $W = 5$ .

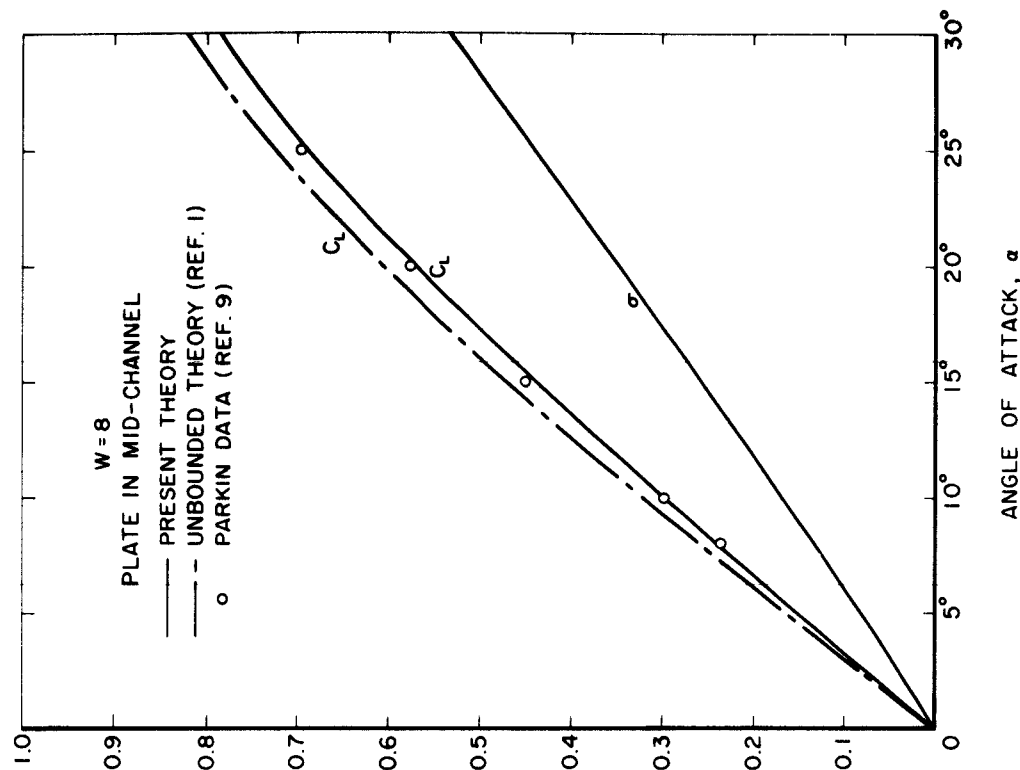


Fig. 9 Comparison of  $C_L$  from the present theory with the unbounded theory and experimental data from Parkin for a plate located mid-channel in a channel of  $W = 8$ .

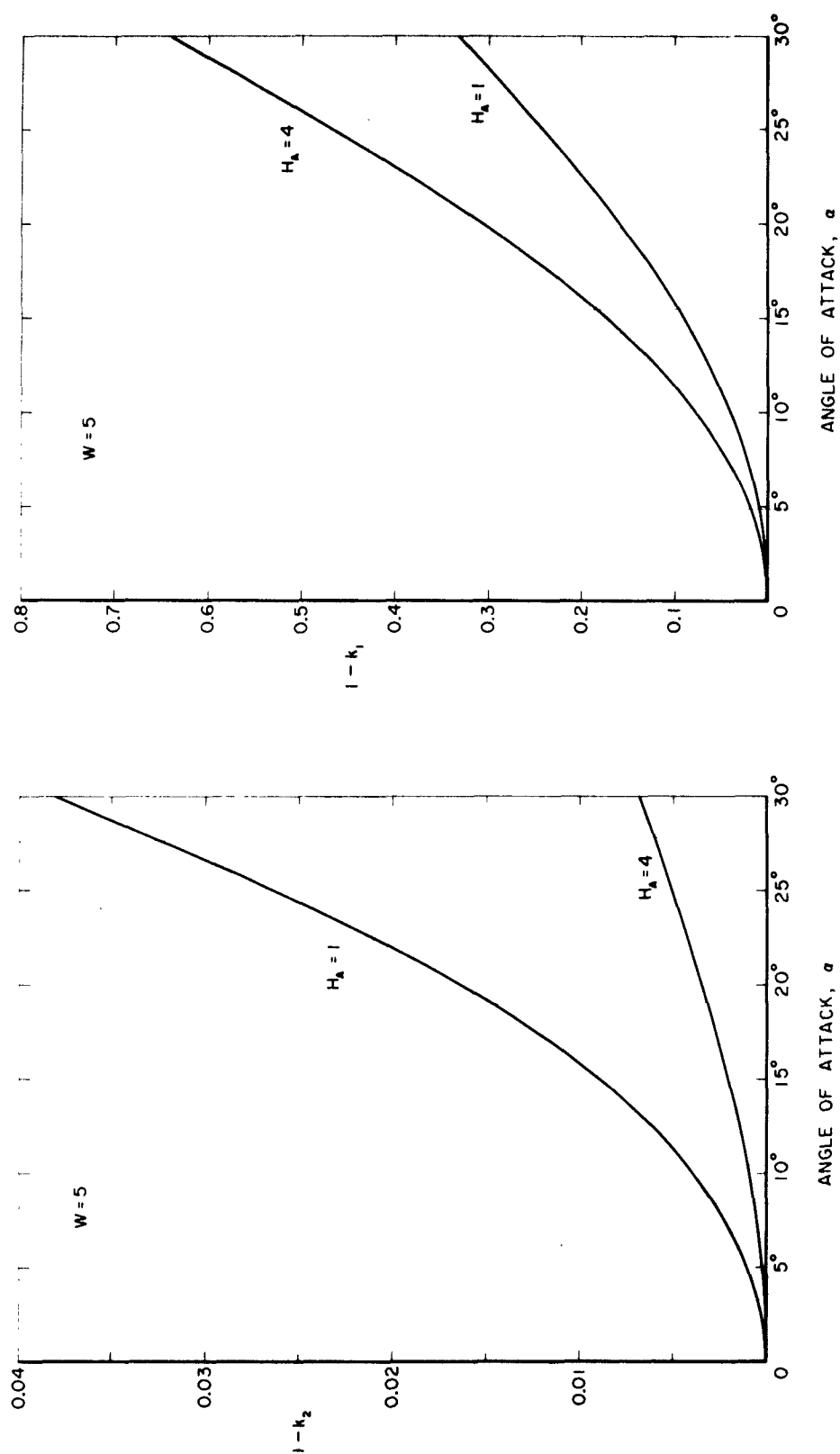


Fig. 10 Effect of channel width on (a) the drag coefficient and (b) the choking cavitation number for a flat plate located mid-channel at various angles of attack.



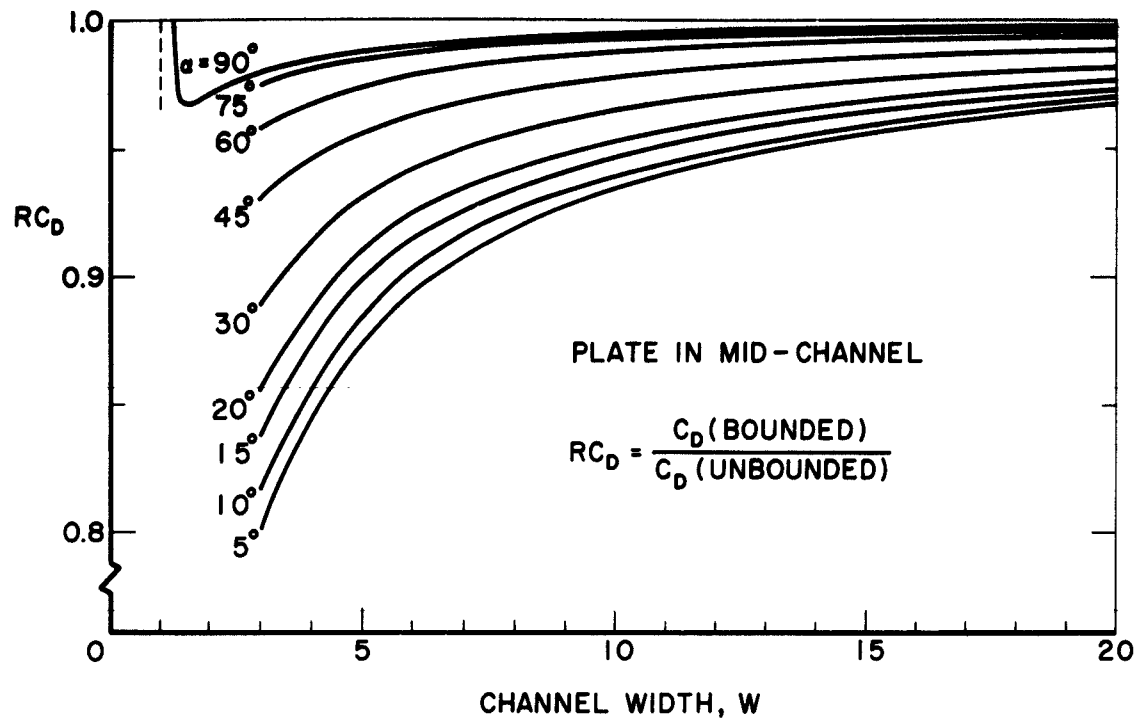


Fig. 11 The ratio of  $C_D$  (bounded) to  $C_D$  (unbounded) versus  $W$  for a flat plate located mid-channel.

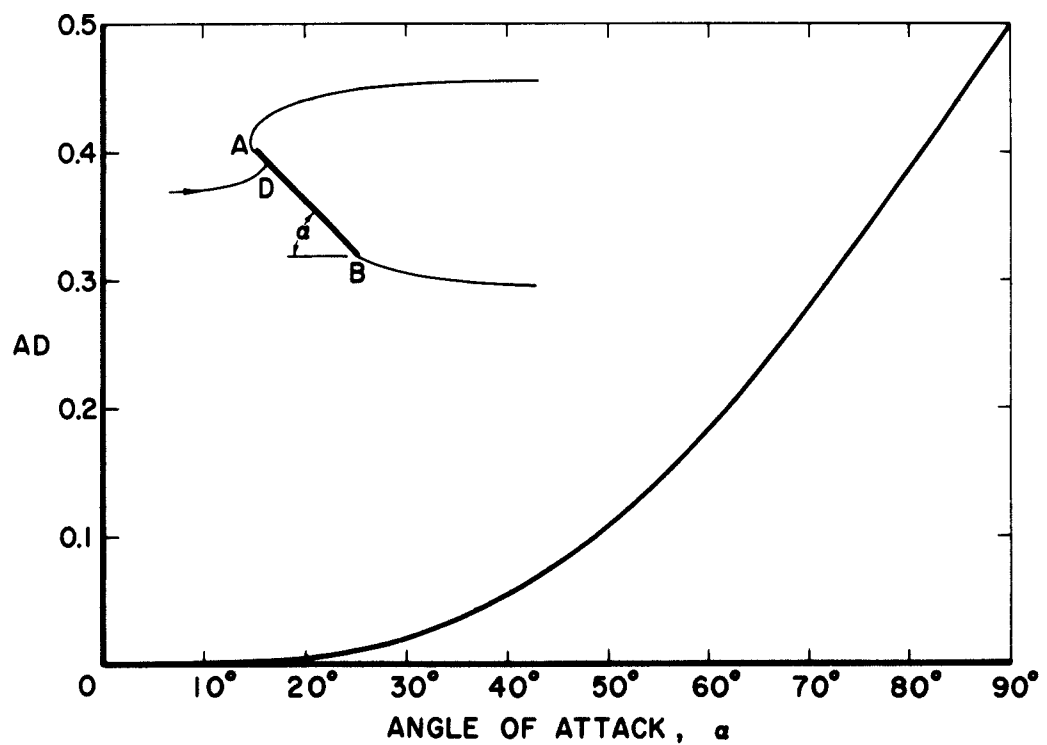


Fig. 12 Distance of stagnation point from the leading edge for  $W = 5$  and the plate in mid-channel.

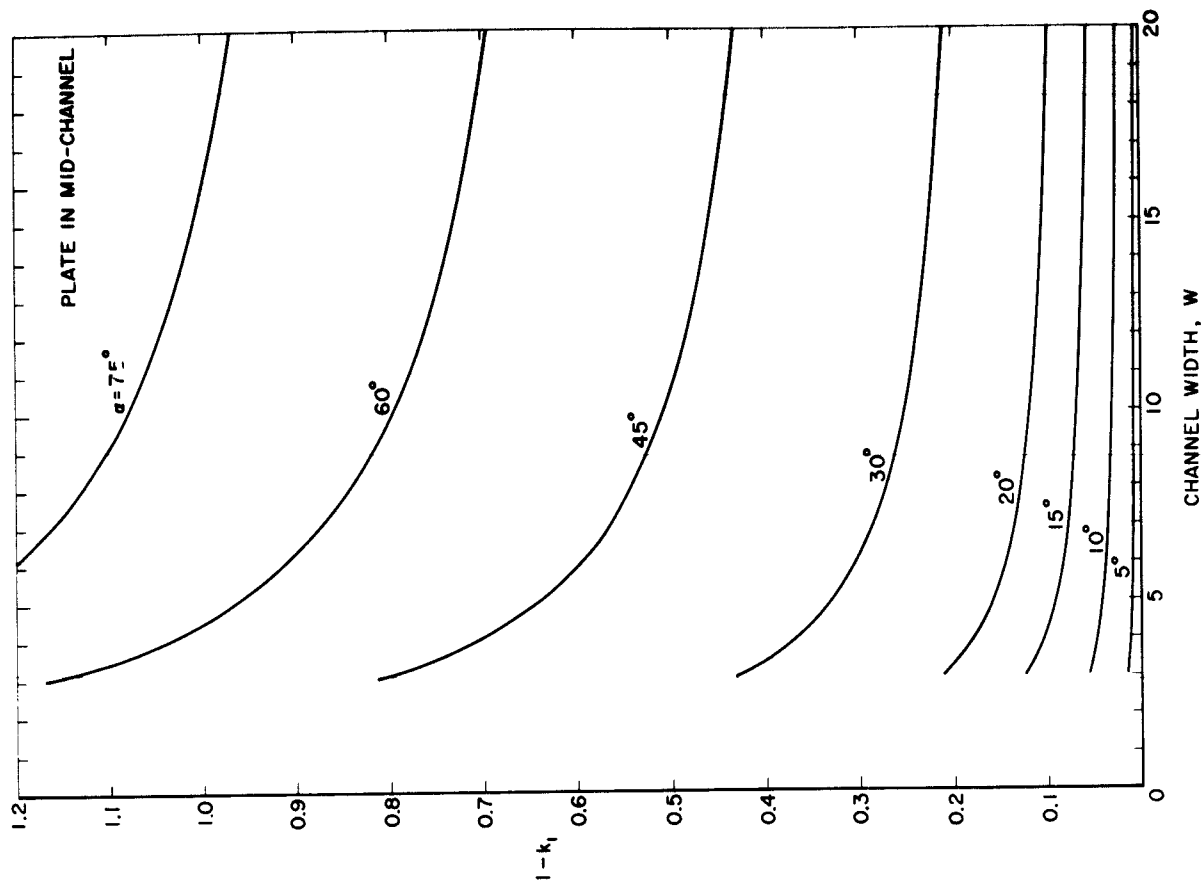
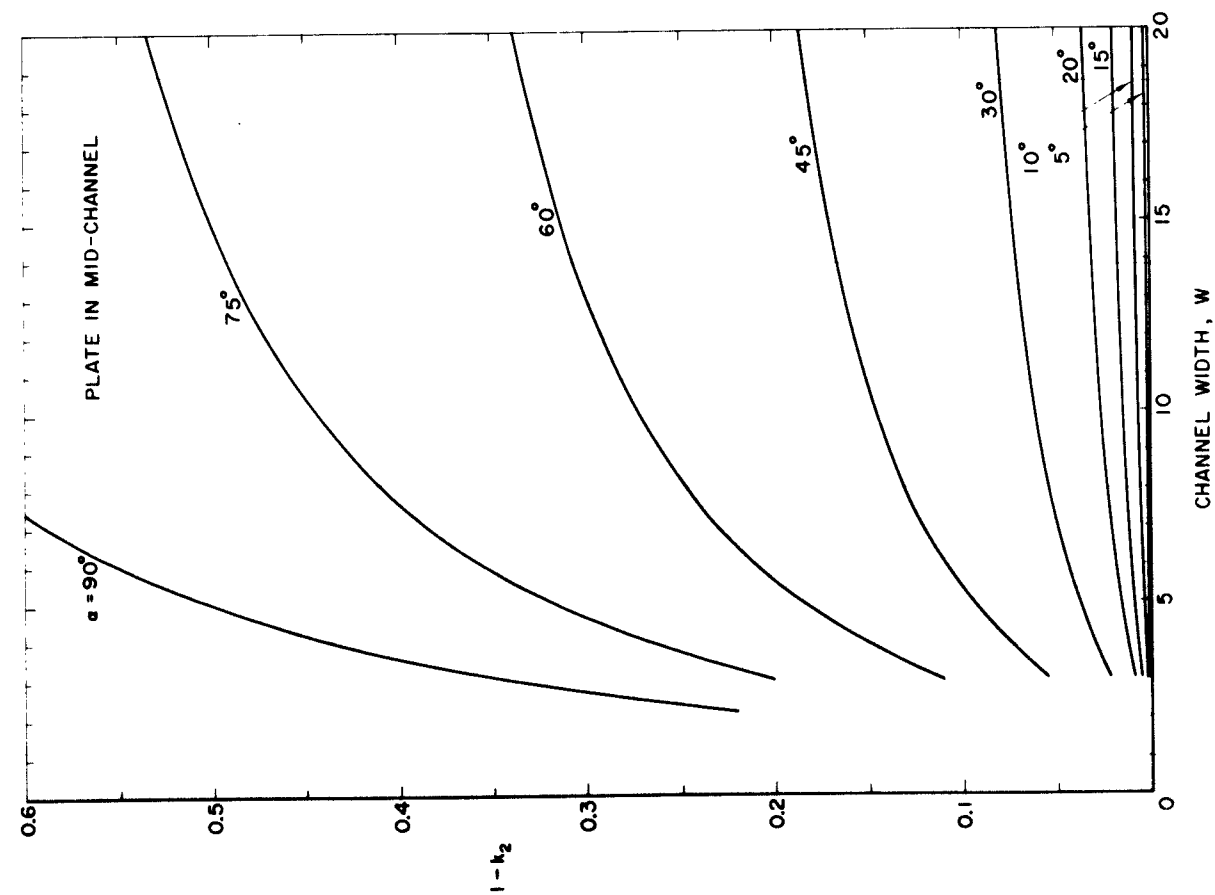


Fig. A-1 Effect of channel width and angle of attack on the transformation parameters (a)  $k_2$  and (b)  $k_1$  for a flat plate located mid-channel.

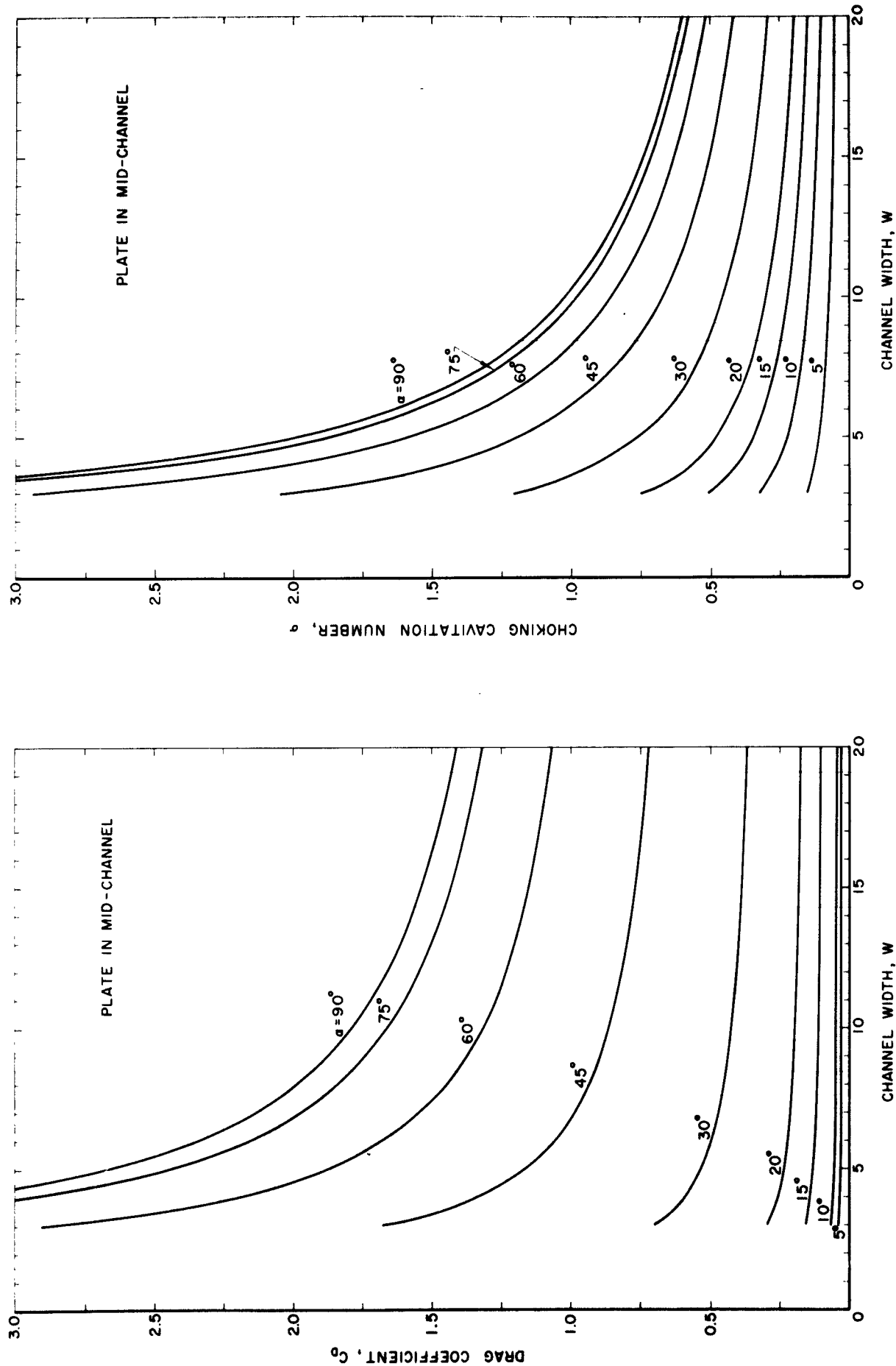


Fig. A-2 Effect of angle of attack and plate position on the transformation parameters (a)  $k_2$  and (b)  $k_1$  for a flat plate in two off-center positions  $H_A = 1$  and 4, in a channel of  $W = 5$ .

**DISTRIBUTION LIST FOR UNCLASSIFIED TECHNICAL REPORTS**

**ISSUED UNDER**

**CONTRACT Nonr-220(41)**

**(Single copies unless otherwise specified)**

Chief of Naval Research  
Department of the Navy  
Washington 25, D.C.  
Attn: Codes 438 (3)

461  
463  
466

Commanding Officer  
Office of Naval Research  
Branch Office  
495 Summer Street  
Boston 10, Massachusetts

Commanding Officer  
Office of Naval Research  
Branch Office  
207 West 24th Street  
New York 11, New York

Commanding Officer  
Office of Naval Research  
Branch Office  
1030 East Green Street  
Pasadena, California

Commanding Officer  
Office of Naval Research  
Branch Office  
1000 Geary Street  
San Francisco 9, California

Commanding Officer  
Office of Naval Research  
Branch Office  
Box 39, Navy No. 100  
Fleet Post Office  
New York, New York (25)

Director  
Naval Research Laboratory  
Washington 25, D. C.  
Attn: Code 2027 (6)

Chief, Bureau of Naval Weapons  
Department of the Navy  
Washington 25, D. C.  
Attn: Codes RUAW-r  
RRRE  
RAAD  
RAAD-222  
DIS-42

Commander  
U. S. Naval Ordnance Test Station  
China Lake, California  
Attn: Code 753

Chief, Bureau of Ships  
Department of the Navy  
Washington 25, D. C.

Attn: Codes 310  
312  
335  
420  
421  
440  
442  
449

Chief, Bureau of Yards and Docks  
Department of the Navy  
Washington 25, D. C.  
Attn: Code D-400

Commanding Officer and Director  
David Taylor Model Basin  
Washington 7, D. C.

Attn: Codes 108  
142  
500  
513  
520  
525  
526  
526A  
530  
533  
580  
585  
589  
591  
591A  
700

Commander  
U.S. Naval Ordnance Test Station  
Pasadena Annex  
3202 E. Foothill Blvd.  
Pasadena 8, California  
Attn: Code P-508

Commander  
Planning Department  
Portsmouth Naval Shipyard  
Portsmouth, New Hampshire

Commander  
Planning Department  
Boston Naval Shipyard  
Boston 29, Massachusetts

Commander  
Planning Department  
Pearl Harbor Naval Shipyard  
Navy No. 128, Fleet Post Office  
San Francisco, California

Commander  
Planning Department  
San Francisco Naval Shipyard  
San Francisco 24, California

Commander  
Planning Department  
Mare Island Naval Shipyard  
Vallejo, California

Commander  
Planning Department  
New York Naval Shipyard  
Brooklyn 1, New York

Commander  
Planning Department  
Puget Sound Naval Shipyard  
Bremerton, Washington

Commander  
Planning Department  
Philadelphia Naval Shipyard  
U. S. Naval Base  
Philadelphia 12, Pennsylvania

Commander  
Planning Department  
Norfolk Naval Shipyard  
Portsmouth, Virginia

Commander  
Planning Department  
Charleston Naval Shipyard  
U. S. Naval Base  
Charleston, South Carolina

Commander  
Planning Department  
Long Beach Naval Shipyard  
Long Beach 2, California

Commander  
Planning Department  
U. S. Naval Weapons Laboratory  
Dahlgren, Virginia

Commander  
U. S. Naval Ordnance Laboratory  
White Oak, Maryland

Dr. A. V. Hershey  
Computation and Exterior  
Ballistics Laboratory  
U. S. Naval Weapons Laboratory  
Dahlgren, Virginia

Superintendent  
U. S. Naval Academy  
Annapolis, Maryland  
Attn: Library

Superintendent  
U. S. Naval Postgraduate School  
Monterey, California

Commandant  
U. S. Coast Guard  
1300 E. Street, N. W.  
Washington, D. C.

Secretary Ship Structure Committee  
U. S. Coast Guard Headquarters  
1300 E Street, N. W.  
Washington, D. C.

Commander  
Military Sea Transportation Service  
Department of the Navy  
Washington 25, D. C.

U. S. Maritime Administration  
GAO Building  
441 G Street, N. W.  
Washington, D. C.  
Attn: Division of Ship Design  
Division of Research

Superintendent  
U. S. Merchant Marine Academy  
Kings Point, Long Island, New York  
Attn: Capt. L. S. McCready  
(Dept. of Engineering)

Commanding Officer and Director  
U. S. Navy Mine Defense Laboratory  
Panama City, Florida

Commanding Officer  
NROTC and Naval Administrative  
Massachusetts Institute of Technology  
Cambridge 39, Massachusetts

U. S. Army Transportation Research and  
Development Command  
Fort Eustis, Virginia  
Attn: Marine Transport Division

Mr. J. B. Parkinson  
National Aeronautics and Space  
Administration  
1512 H Street, N. W.  
Washington 25, D. C.

Director  
Langley Research Center  
Langley Station  
Hampton, Virginia  
Attn: Mr. I. E. Garrick  
Mr. D. J. Marten

Director Engineering Sciences Division  
National Science Foundation  
1951 Constitution Avenue, N. W.  
Washington 25, D. C.

Director  
National Bureau of Standards  
Washington 25, D. C.  
Attn: Fluid Mechanics Division  
(Dr. G. B. Schubauer)  
Dr. G. H. Keulegan  
Dr. J. M. Franklin

Defense Documentation Center  
Cameron Station  
Alexandria, Virginia (20)  
Office of Technical Services  
Department of Commerce  
Washington 25, D. C.

California Institute of Technology  
Pasadena 4, California  
Attn: Professor M. S. Plesset  
Professor T. Y. Wu  
Professor A. J. Acosta

University of California  
Department of Engineering  
Los Angeles 24, California  
Attn: Dr. A. Powell

Director  
Scripps Institute of Oceanography  
University of California  
La Jolla, California

Professor M. L. Albertson  
Department of Civil Engineering  
Colorado A and M College  
Fort Collins, Colorado

Professor J. E. Cermak  
Department of Civil Engineering  
Colorado State University  
Fort Collins, Colorado

Professor W. R. Sears  
Graduate School of Aeronautical Engineering  
Cornell University  
Ithaca, New York

State University of Iowa  
Iowa Institute of Hydraulic Research  
Iowa City, Iowa  
Attn: Dr. H. Rouse  
Dr. L. Landweber

Massachusetts Institute of Technology  
Cambridge 39, Massachusetts  
Attn: Department of Naval Architecture  
and Marine Engineering  
Professor A. T. Ippen

Harvard University  
Cambridge 38, Massachusetts  
Attn: Professor G. Birkhoff  
(Dept. of Mathematics)  
Professor G. F. Carrier  
(Dept. of Mathematics)

University of Michigan  
Ann Arbor, Michigan  
Attn: Professor R. B. Couch  
(Dept. of Naval Architecture)  
Professor W. W. Willmarth  
(Aero. Engineering Department)

Dr. L. G. Straub, Director  
St. Anthony Falls Hydraulic Laboratory  
University of Minnesota  
Minneapolis 14, Minnesota  
Attn: Mr. J. N. Wetzel  
Professor B. Silberman

Professor J. J. Foody  
Engineering Department  
New York State University Maritime College  
Fort Schuyler, New York

New York University  
Institute of Mathematical Sciences  
25 Waverly Place  
New York 3, New York  
Attn: Professor J. Keller  
Professor J. J. Stoker

The Johns Hopkins University  
Department of Mechanical Engineering  
Baltimore 18, Maryland  
Attn: Professor S. Corrsin  
Professor O. M. Phillips (2)

Massachusetts Institute of Technology  
Department of Naval Architecture and  
Marine Engineering  
Cambridge 39, Massachusetts  
Attn: Professor M. A. Abkowitz, Head

Dr. G. F. Wislicenus  
Ordnance Research Laboratory  
Pennsylvania State University  
University Park, Pennsylvania  
Attn: Dr. M. Sevik

Professor R. C. DiPrima  
Department of Mathematics  
Rensselaer Polytechnic Institute  
Troy, New York

Director  
Woods Hole Oceanographic Institute  
Woods Hole, Massachusetts

Stevens Institute of Technology  
Davidson Laboratory  
Castle Point Station  
Hoboken, New Jersey  
Attn: Mr. D. Savitsky  
Mr. J. P. Breslin  
Mr. C. J. Henry  
Mr. S. Tsakonas

Webb Institute of Naval Architecture  
Crescent Beach Road  
Glen Cove, New York  
Attn: Professor E. V. Lewis  
Technical Library

Executive Director  
Air Force Office of Scientific Research  
Washington 25, D. C.  
Attn: Mechanics Branch

Commander  
Wright Air Development Division  
Aircraft Laboratory  
Wright-Patterson Air Force Base, Ohio  
Attn: Mr. W. Mykytow, Dynamics  
Branch

Cornell Aeronautical Laboratory  
4455 Genesee Street  
Buffalo, New York  
Attn: Mr. W. Targoff  
Mr. R. White

Massachusetts Institute of Technology  
Fluid Dynamics Research Laboratory  
Cambridge 39, Massachusetts  
Attn: Professor H. Ashley  
Professor M. Landahl  
Professor J. Dugundji

Hamburgische Schiffbau-Versuchsanstalt  
Bramfelder Strasse 164  
Hamburg 33, Germany  
Attn: Dr. H. Schwanecke  
Dr. H. W. Lerbs

Institut für Schiffbau der  
Universität Hamburg  
Berliner Tor 21  
Hamburg 1, Germany  
Attn: Prof. G. P. Weinblum,

Transportation Technical Research Institute  
1-1057, Mejiro-Cho, Toshima-Ku  
Tokyo, Japan

Max-Planck Institut für Stromungsforschung  
Bottingerstrasse 6/8  
Gottingen, Germany  
Attn: Dr. H. Reichardt

Hydro-og Aerodynamisk Laboratorium  
Lyngby, Denmark  
Attn: Professor Carl Prohaska

Shipsmodelltanken  
Trondheim, Norway  
Attn: Professor J. K. Lunde  
Versuchsanstalt für Wasserbau und  
Schiffbau  
Schleuseninsel im Tiergarten  
Berlin, Germany  
Attn: Dr. S. Schuster, Director  
Dr. Grosse

Technische Hogeschool  
Institut voor Toegepaste Wiskunde  
Julianalaan 132  
Delft, Netherlands  
Attn: Professor R. Timman

Bureau D'Analyse et de Recherche  
Appliquees  
47 Avenue Victor Bresson  
Issy-Les-Moulineaux  
Seine, France  
Attn: Professor Siestrunck

Netherlands Ship Model Basin  
Wageningen, The Netherlands  
Attn: Dr. Ir. J. D. vanManen

National Physical Laboratory  
Teddington, Middlesex, England  
Attn: Mr. A. Silverleaf, Superintendent  
Ship Division  
Head, Aerodynamics Division

Head, Aerodynamics Department  
Royal Aircraft Establishment  
Farnborough, Hants, England  
Attn: Mr. M. O. W. Wolfe

Dr. S. F. Hoerner  
148 Busteed Drive  
Midland Park, New Jersey

Boeing Airplane Company  
Seattle Division  
Seattle, Washington  
Attn: Mr. M. J. Turner

Electric Boat Division  
General Dynamics Corporation  
Groton, Connecticut  
Attn: Mr. Robert McCandliss

General Applied Sciences Labs., Inc.  
Merrick and Stewart Avenues  
Westbury, Long Island, New York  
Gibbs and Cox, Inc.  
21 West Street  
New York, New York

Lockheed Aircraft Corporation  
Missiles and Space Division  
Palo Alto, California  
Attn: R. W. Kermeen

Grumman Aircraft Engineering Corp.  
Bethpage, Long Island, New York  
Attn: Mr. E. Baird  
Mr. E. Bower  
Mr. W. P. Carl

Midwest Research Institute  
425 Volker Blvd.  
Kansas City 10, Missouri  
Attn: Mr. Zeydel

Director, Department of Mechanical  
Sciences  
Southwest Research Institute  
8500 Culebra Road  
San Antonio 6, Texas  
Attn: Dr. H. N. Abramson  
Mr. G. Ransleben  
Editor, Applied Mechanics  
Review

Convair  
A Division of General Dynamics  
San Diego, California  
Attn: Mr. R. H. Oversmith  
Mr. H. T. Brooke

Hughes Tool Company  
Aircraft Division  
Culver City, California  
Attn: Mr. M. S. Harned

Hydronautics, Incorporated  
Pindell School Road  
Howard County  
Laurel, Maryland  
Attn: Mr. Phillip Eisenberg

Rand Development Corporation  
13600 Deise Avenue  
Cleveland 10, Ohio  
Attn: Dr. A. S. Iberall

U. S. Rubber Company  
Research and Development Department  
Wayne, New Jersey  
Attn: Mr. L. M. White

Technical Research Group, Inc.  
Route 110  
Melville, New York, 11749  
Attn: Mr. Jack Kotik

Mr. C. Wigley  
Flat 102  
6-9 Charterhouse Square  
London, E. C. 1, England

AVCO Corporation  
Lycoming Division  
1701 K Street, N. W.  
Apt. No. 904  
Washington, D. C.  
Attn: Mr. T. A. Duncan

Mr. J. G. Baker  
Baker Manufacturing Company  
Evansville, Wisconsin

Curtiss-Wright Corporation Research  
Division  
Turbomachinery Division  
Quehanna, Pennsylvania  
Attn: Mr. George H. Pedersen

Dr. Blaine R. Parkin  
AiResearch Manufacturing Corporation  
9851-9951 Sepulveda Boulevard  
Los Angeles 45, California

The Boeing Company  
Aero-Space Division  
Seattle 24, Washington  
Attn: Mr. R. E. Bateman  
(Internal Mail Station 46-74)

Lockheed Aircraft Corporation  
California Division  
Hydrodynamics Research  
Burbank, California  
Attn: Mr. Bill East

National Research Council  
Montreal Road  
Ottawa 2, Canada  
Attn: Mr. E. S. Turner

The Rand Corporation  
1700 Main Street  
Santa Monica, California  
Attn: Technical Library

Stanford University  
Department of Civil Engineering  
Stanford, California  
Attn: Dr. Byrne Perry  
Dr. E. Y. Hsu

Dr. Hirsh Cohen  
IBM Research Center  
P. O. Box 218  
Yorktown Heights, New York

Mr. David Wellinger  
Hydrofoil Projects  
Radio Corporation of America  
Burlington, Massachusetts

Food Machinery Corporation  
P. O. Box 367  
San Jose, California  
Attn: Mr. G. Tedrew

Dr. T. R. Goodman  
Oceanics, Inc.  
Technical Industrial Park  
Plainview, Long Island, New York



Professor Brunelle  
Department of Aeronautical Engineering  
Princeton University  
Princeton, New Jersey

Commanding Officer  
Office of Naval Research Branch Office  
219 S. Dearborn Street  
Chicago 1, Illinois 60604

University of Colorado  
Aerospace Engineering Sciences  
Boulder, Colorado  
Attn: Prof. M. S. Uberoi

The Pennsylvania State University  
Dept. of Aeronautical Engineering  
Ordnance Research Laboratory  
P. O. Box 30  
State College, Pennsylvania  
Attn: Professor J. William Holl

Institut für Schiffbau der Universität Hamburg  
Lammersbeth 90  
2 Hamburg 33, Germany  
Attn: Dr. O. Grim

Technische Hogeschool  
Laboratorium voor Scheepsbouwkunde  
Mekelweg 2, Delft, Netherlands  
Attn: Professor Ir. J. Gerritsma

Unclassified  
Security Classification

| DOCUMENT CONTROL DATA - R&D   |   |  |
|---|---|--|
| (Security classification of title, body of abstract and indexing annotation must be entered when the overall report is classified)  |   |  |
| 1. ORIGINATING ACTIVITY (Corporate author)<br>Office of Naval Research, Dept. of the Navy<br>Washington, D. C.  |   | 2a. REPORT SECURITY CLASSIFICATION<br>Unclassified |
|   |   | 2b. GROUP  |
| 3. REPORT TITLE<br><br>The Wall Effect in Cavity Flow   |   |  |
| 4. DESCRIPTIVE NOTES (Type of report and inclusive dates)<br>Final  |   |  |
| 5. AUTHOR(S) (Last name, first name, initial)<br><br>Ai, Daniel K. and Harrison, Zora L.  |   |  |
| 6. REPORT DATE<br>April, 1965   | 7a. TOTAL NO. OF PAGES<br>20  | 7b. NO. OF REFS<br>9                               |
| 8a. CONTRACT OR GRANT NO.<br>Nonr-220(41) 61260   | 9a. ORIGINATOR'S REPORT NUMBER(S)<br><br>E-111.3                                  |  |
| b. PROJECT NO.<br><br>c.<br><br>d.  | 9b. OTHER REPORT NO(S) (Any other numbers that may be assigned this report)       |  |
| 10. AVAILABILITY/LIMITATION NOTICES<br><br>"Qualified requesters may obtain copies of this report from DDC."  |   |  |
| 11. SUPPLEMENTARY NOTES   | 12. SPONSORING MILITARY ACTIVITY<br>Office of Naval Research<br>Washington, D. C. |  |
| 13. ABSTRACT<br><br>A nonlinear theory for the calculation of the flow field of an oblique flat plate under blockage condition is given using the techniques of integral equations. Numerical results are obtained with the aid of a high speed digital computer for the plate situated mid-channel at values of the angle of attack from 5° to 90° and the channel-width-chord ratio from 3 to 20. Also obtained are results for the plate situated at two different off-center positions for a channel width-chord ratio of 5 and angles of attack less than 30°. |   |  |

DD FORM 1 JAN 64 1473

Unclassified  
Security Classification

Unclassified

Security Classification

| 14 | KEY WORDS | LINK A |    | LINK B |    | LINK C |    |
|----|-----------|--------|----|--------|----|--------|----|
|    |           | ROLE   | WT | ROLE   | WT | ROLE   | WT |
|    |           |        |    |        |    |        |    |

## INSTRUCTIONS

1. **ORIGINATING ACTIVITY:** Enter the name and address of the contractor, subcontractor, grantee, Department of Defense activity or other organization (*corporate author*) issuing the report.

2a. **REPORT SECURITY CLASSIFICATION:** Enter the overall security classification of the report. Indicate whether "Restricted Data" is included. Marking is to be in accordance with appropriate security regulations.

2b. **GROUP:** Automatic downgrading is specified in DoD Directive 5200.10 and Armed Forces Industrial Manual. Enter the group number. Also, when applicable, show that optional markings have been used for Group 3 and Group 4 as authorized.

3. **REPORT TITLE:** Enter the complete report title in all capital letters. Titles in all cases should be unclassified. If a meaningful title cannot be selected without classification, show title classification in all capitals in parenthesis immediately following the title.

4. **DESCRIPTIVE NOTES:** If appropriate, enter the type of report, e.g., interim, progress, summary, annual, or final. Give the inclusive dates when a specific reporting period is covered.

5. **AUTHOR(S):** Enter the name(s) of author(s) as shown on or in the report. Enter last name, first name, middle initial. If military, show rank and branch of service. The name of the principal author is an absolute minimum requirement.

6. **REPORT DATE:** Enter the date of the report as day, month, year, or month, year. If more than one date appears on the report, use date of publication.

7a. **TOTAL NUMBER OF PAGES:** The total page count should follow normal pagination procedures, i.e., enter the number of pages containing information.

7b. **NUMBER OF REFERENCES:** Enter the total number of references cited in the report.

8a. **CONTRACT OR GRANT NUMBER:** If appropriate, enter the applicable number of the contract or grant under which the report was written.

8b, &, & 8d. **PROJECT NUMBER:** Enter the appropriate military department identification, such as project number, subproject number, system numbers, task number, etc.

9a. **ORIGINATOR'S REPORT NUMBER(S):** Enter the official report number by which the document will be identified and controlled by the originating activity. This number must be unique to this report.

9b. **OTHER REPORT NUMBER(S):** If the report has been assigned any other report numbers (*either by the originator or by the sponsor*), also enter this number(s).

10. **AVAILABILITY/LIMITATION NOTICES:** Enter any limitations on further dissemination of the report, other than those

imposed by security classification, using standard statements such as:

- (1) "Qualified requesters may obtain copies of this report from DDC."
- (2) "Foreign announcement and dissemination of this report by DDC is not authorized."
- (3) "U. S. Government agencies may obtain copies of this report directly from DDC. Other qualified DDC users shall request through \_\_\_\_\_."
- (4) "U. S. military agencies may obtain copies of this report directly from DDC. Other qualified users shall request through \_\_\_\_\_."
- (5) "All distribution of this report is controlled. Qualified DDC users shall request through \_\_\_\_\_."

If the report has been furnished to the Office of Technical Services, Department of Commerce, for sale to the public, indicate this fact and enter the price, if known.

11. **SUPPLEMENTARY NOTES:** Use for additional explanatory notes.

12. **SPONSORING MILITARY ACTIVITY:** Enter the name of the departmental project office or laboratory sponsoring (*paying for*) the research and development. Include address.

13. **ABSTRACT:** Enter an abstract giving a brief and factual summary of the document indicative of the report, even though it may also appear elsewhere in the body of the technical report. If additional space is required, a continuation sheet shall be attached.

It is highly desirable that the abstract of classified reports be unclassified. Each paragraph of the abstract shall end with an indication of the military security classification of the information in the paragraph, represented as (TS), (S), (C), or (U).

There is no limitation on the length of the abstract. However, the suggested length is from 150 to 225 words.

14. **KEY WORDS:** Key words are technically meaningful terms or short phrases that characterize a report and may be used as index entries for cataloging the report. Key words must be selected so that no security classification is required. Identifiers, such as equipment model designation, trade name, military project code name, geographic location, may be used as key words but will be followed by an indication of technical context. The assignment of links, rules, and weights is optional.

Unclassified

Security Classification